INTERNATIONAL JOURNAL OF APPLIED
SCIENCE ENGINEERING AND MANAGEMENT

IJASEM

E-Mail :
editor.ijasem@gmail.com
editor@ijasem.org

www.ijasem.org

Modified Z-source Integrated PV/Grid/EV DC Charger/Inverter Modeling, Design, Control, and Implementation

N.Mahesh[1],M.Venkateshwar Rao.[2],Y.Prakash[3],R.Shankar[4],

Abstract— *Sun based Energy has been the most well known wellsprings of sustainable power source for private and semi business applications. Vacillations of sunlight based vitality gathered because of climatic conditions can be moderated through vitality stockpiling frameworks. Sun oriented vitality can likewise be utilized to charge electric vehicle batteries to lessen the reliance on the network. One of the prerequisites for a converter for such applications is to have a decreased number of changes organizes and give seclusion. Z-source inverter (ZSI) topology can expel various stages and accomplish voltage lift and DC-AC power transformation in a solitary stage. The utilization of latent parts additionally exhibits a chance to coordinate vitality stockpiling frameworks (ESS) into them. This paper presents demonstrating, plan and activity of an altered Z-source inverter (MZSI) incorporated with a split essential secluded battery charger for DC charging of electric vehicles (EV) batteries. Reenactment and exploratory outcomes have been displayed for the evidence of idea of the activity of the proposed converter.*

I. INTRODUCTION

Charging of electric vehicles at present heavily involve the use AC grid. The various methods of charging exclusivey use AC grid, such as wireless charging or plug-in charging can still cause pollution irrespective of how highly efficient the topology is. The amount of fossil fuels that are consumed to generate the energy to charge an electric vehicle gives a clearer picture of the carbon footprint that is left behind while charging an electric vehicle. To achieve lower carbon footprints, one of the ways is to integrated renewable energy sources into a charging infrastructure to reduce the dependency on the AC grid. A major requirement for designing an EV battery charger isthe use of isolation transformers in the converter topologies, to provide galvanic isolation at the user end from the rest of the high voltage (HV) system as a safety measure [1]. The galvanic isolation can be provided either on the AC grid side or on the charger side. The size of the isolation transformer on the grid side is usually much larger than the one on the charger side [2]. Due to the improvement in

semiconductor technology, high frequency switching facilitates the use of smaller size transformers for galvanic isolation. Photovoltaic grid interconnected systems have been used in the past for commercial charging infrastructure [3]. These systems reduce the dependency of the charging infrastructure on the AC grid. The use of solar and grid interconnected system is an attractive solution for residential charging systems for EVs. For systems upto 10 kW, single phase inverters can be used for residential applications [4][5]. For interconnection of the residential solar PV to the grid, various isolated and non isolated topologies are available with multiple stages [4]- [6]. Residential photovoltaic systems for EV charging require features such as isolation and voltage boost capability to match the solar PV array voltage to the grid voltage requirements. The ZSI topology was first introduced in [7]. It has an ability to buck or boost and invert the input DC voltage in a single stage.

*Professor[1], Assistant Professor[2,3,4],
Department of EEE Engineering,
Pallavi Engineering College,
Mail.id: nimmalamahesh01@gmail.com ,Mail.id:venkasnmpkmm@gmail.com,
Kuntloor(V),Hayathnagar(M),Hyderabad,R.R.Dist.-501505.*

It has gained tremendous interest in photovoltaic-grid connected applications. The ZSI topology uses two capacitors and two inductors to boost the input DC voltage to match the inverter side AC output voltage requirements. The operation of a ZSI is heavily dependent on the passive components. It presents an opportunity to integrate energy storage units into such a system.

In this paper a proof of concept of a single phase MZSI based solar grid connected charger has been presented as an application towards a string inverter configuration. In section II, the basic operation principle for a ZSI have been discussed along with the component design. Section III, discusses the sizing of components, modeling and control of the converter. Section IV, presents the simulation results for the operation of a 3.3 kW proposed inverter charger and results from an experimental setup built as a proof of concept. Section V, presents the conclusion.
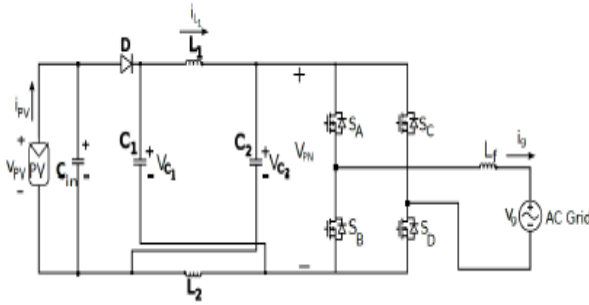

Fig. 1. Schematic of a Photovoltaic/AC grid inter-connected Z-source Inverter(ZSI)

II. TRADITIONAL ZSI

The ZSI topology, shown in Fig.1, utilizes two modes of operation: the shoot through state and the non shoot through state [7]. For symmetrical operations,

$$i_L = i_{L1} = i_{L2} \qquad (1)$$

$$V_C = V_{C1} = V_{C2} \qquad (2)$$

From Fig.1, in the shoot through state, all four switches, S1, S3, S2 and S4, are conducting at the same time. The duration of this shoot through state is described by the duty cycle D0 and the switching frequency FSW. The shoot through state can be implemented by a modified PWM technique presented in [7]. Therefore, the two capacitor voltages are expressed as [7]:

$$V_C = \frac{1 - D_0}{1 - 2D_0} v_{pv} \qquad (3)$$

Thus, maintaining a higher peak voltage at the input of the DC link, VPN. The peak DC link voltage, VP^N, is given by [7]:

$$\hat{V_{PN}} = \frac{1}{1 - 2D_0} v_{pv} \qquad (4)$$

The power balance equation between the DC and AC side of the ZSI is expressed as [7],

$$(1 - D_0)\hat{V_{PN}} I_{PN} = i_{grms} v_{grms} \qquad (5)$$

where IPN and VP^N are the peak DC link current and voltage. The peak AC voltage of the ZSI is [7]:

$$V_g = M\hat{V_{PN}} \qquad (6)$$

where the M is the modulation index, grid voltage, vg=Vgsin!t and the grid current ig=Igsin(!t+_). For _=0 for grid connected applications. From equation (11) and (13) the RMS of the output AC voltage of the ZSI is [7]:

$$V_{grms} = \frac{M v_{pv}}{\sqrt{2}(1 - 2D_0)} \qquad (7)$$

III. COMPONENT SIZING, MODELING AND CONTROL OF PROPOSED MZSI

Fig. 2 shows a modified Z source inverter has been proposed having an integrated charger. The two capacitors C1 and C2 from Fig.1 are split and each of them act as one of the legs of one of the two primaries of the split primary isolated half bridge converter. The MOSFET SR allows bidirectional operation of the MZSI when required. The diode DPV blocks the reverse flow of current back into the PV. Rin is the internal resistance of the input capacitor Cin. For symmetrical operation of the MZSI, a split primary isolated DC to DC converter has been proposed for the integration of the charger side into the ZSI. The split primaries contain two half bridge converter (HBC) primaries isolated from a single full bridge secondary through a high frequency transformer. The HBC primaries and the secondaries are operated at 50% duty cycle in open loop. The output current of the secondary is connected to a energy storage unit such as a lithium-ion (Li-ion) battery. The energy storage unit clamps its own voltage, vB, across
the input of the HBC primaries, VC, such that,

$$V_C = 2v_B \qquad (8)$$

A. Maximum Shoot Through Duty Ratio,D0max
As a result of the energy storage unit being connected across the capacitors, the maximum shoot through duty ratio, D0max is calculated based on the

minimum input voltage, vpvmin and the maximum battery voltage, VBmax connected across the capacitors and is expressed as:

$$D_{0max} = \frac{2V_{Bmax} - v_{pvmin}}{4V_{Bmax} - v_{pvmin}} \qquad (9)$$

SAE J1772 standard defines the standard battery voltages for DC charging between 200V-500V.

B. Inductor L1 and L2 design
The inductors L1 and L2 are sized for high frequency peak to peak current ripple assumed between 15-25% of the

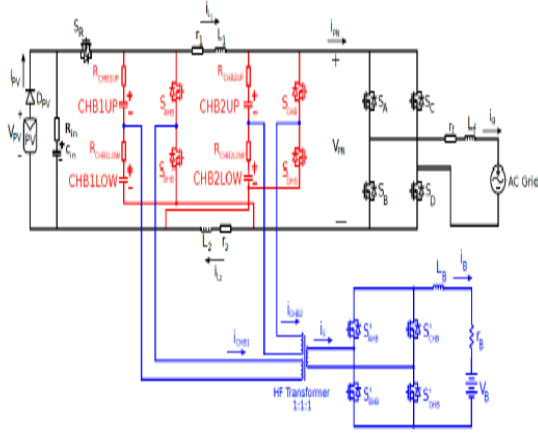
Fig. 2. Detailed Schematic of Proposed MZSI

inductor current during the shoot-through time interval D0T/2as follow [8]:

$$L_1 = L_2 = \frac{V_{Cmax}D_{0max}}{2\Delta i_L f} \qquad (10)$$

C. Capacitor C1 and C2 design
The capacitors are sized to absorb the second order harmonic component in the capacitor voltages as follow [8]:

$$C_1 = C_2 = \frac{P}{2\omega \Delta V_C V_C} \qquad (11)$$

where VC is the average voltage across the capacitors VC1 and VC2 and _VC is the predetermined voltage ripple limit. ! is the second order harmonics expressed in rad/s. In single phase Z source inverters, oversized electrolytic capacitors for second order harmonics suppression can result in a bulky system. A DC side Active Power Filter(APF) proposed in [9], can be used to reduce the capacitance required. It operates independent of the operation of the MZSI. For the proposed topology, maximum capacitor voltage rating is equal to at least twice the peak voltage of the energy storage device clamped across it.

D. Average Modeling of the Integrated Half-Bridge DCDC Converter Charger

When a energy storage unit is connected to the secondary side of the charger then each of the split primaries operates alternately and supplies half the required battery current. Each of the primaries of the DC-DC converter is connected across the capacitors of either legs. The voltage across the capacitors is defined by the equation (15). The detailed average modeling of the split primary DC-DC converter is explained in [10].Each of the two primaries can be represented using a RLE circuit connected parallel to each of the capacitor, C1 and C2, as shown in the simplified equivalent model of the the Fig.4.
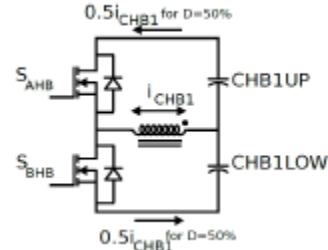

Fig. 3. Schematic of one the Primary across CHB1 operating at 50% duty cycle.

E. State Space Average Modeling of the Single Stage
Inverter Charger The detailed state space average modeling was presented in [10]. The equivalent diagram of the modeled MZSI is shown in the Fig. 4, During the non shoot-through state, the KVL equation is given by:

$$L\frac{di_L}{dt} = v_{pv} - i_L r + R_{HB} + (2\tilde{i_g} + \frac{i_B}{2})R_{HB} - V_C \quad (12)$$

The KCL equation is:

$$C\frac{dV_C}{dt} = i_L - \tilde{i_g} - \frac{i_B}{4} \qquad (13)$$

During the shoot-through state, the KVL equation is:

$$L\frac{di_L}{dt} = V_C - i_L(R_{HB} + r) - \frac{i_B}{2}R_{HB} \qquad (14)$$

The KCL equation is written as:
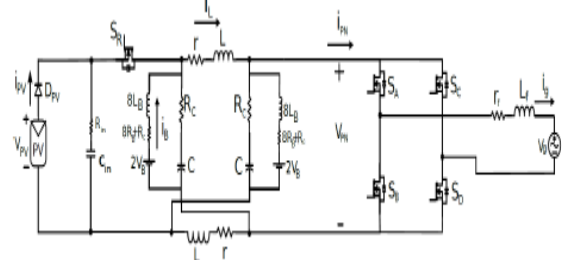
$$C\frac{dV_C}{dt} = -i_L - \frac{i_B}{4} \qquad (15)$$

Fig. 4. Equivalent Model of the proposed Modified Z-source Inverter(MZSI) with battery

From equation (12)-(15), state space equations for the entire system can be written as:

60

$$\begin{bmatrix} \dot{i}_L \\ \dot{V}_C \\ \dot{i}_B \end{bmatrix} = \begin{bmatrix} \frac{-(r+2R_{HB})}{L} & -\frac{1-2D_0}{L} & \frac{(1-2D_0)}{2}R_{HB} \\ \frac{1-2D_0}{C} & 0 & -\frac{1}{4C} \\ \frac{1-2D_0}{L_B}R_{HB} & \frac{1}{2L_B} & -\frac{R_{HB}+R_B}{2L_B} \end{bmatrix} \begin{bmatrix} i_L \\ V_C \\ i_B \end{bmatrix}$$
$$+ \begin{bmatrix} \frac{2(1-D_0)R_{HB}}{L} \\ -\frac{1-D_0}{C} \\ -\frac{(1-D_0)R_{HB}}{L_B} \end{bmatrix} [i_d]$$
$$+ \begin{bmatrix} \frac{(1-D_0)}{L} \\ 0 \\ 0 \end{bmatrix} [v_{pv}]$$
$$+ \begin{bmatrix} 0 \\ 0 \\ -\frac{1}{L_B} \end{bmatrix} [V_B] \qquad (16)$$

Fig. 4 shows the positive directions of the battery current,

iB, and the grid side AC current, ig.Fig. 5 shows the block diagram for the controller for the proposed MZSI topology. It consists of three loops: the PVcurrent ipv loop, grid current ig loop and the battery current iB loop.
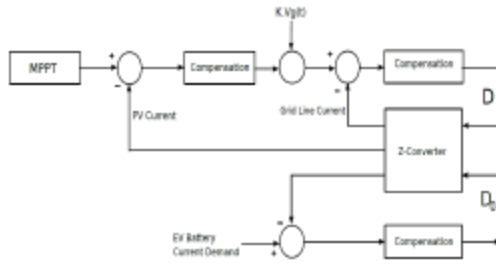

Fig. 5. Block diagram of the Control Scheme Proposed Modified Zsource Inverter Charger

In literature, the ZSI capacitor voltage is controlled to generate the reference current for the H-bridge inverter output

current [11] or generate the shoot through duty ratio D0 [12]. In this paper the reference current is generated by controlling the peak input photovoltaic current [13]. If a stiff voltage VC is connected across either or both capacitors, the shoot through duty ratio, D0, will depend on VC. Since the battery current loop do not require fast dynamic changes battery loop control is the slowest response compared to the input current control. For the battery loop control the transfer function is given by:

$$\frac{I_B(s)}{d_0(s)} = \frac{-sC[4R_{HB}i_L - 2R_{HB}i_d] - [2i_L - i_d]}{2L_BCs^2 + sC[R_{HB} + 2R_B] + 0.25} \qquad (17)$$

A feedforward is added to the battery control loop,

$$FF_B = \frac{2V_B - v_{PV}}{4V_B - v_{PV}} \qquad (18)$$

where VB is the output voltage of the HBC and vPV is the tracked PV voltage. The output AC side current controller should have the fastest response.

F. Energy Management Scheme for the Proposed Converter

Fig. 6 shows a simplified block diagram of the proposed system. When an ESS is integrated into a ZSI, the equation

(5) is modified as follows [14]:

$$v_{PV}i_{PV} = v_b i_b + i_{grms}v_{grms} \qquad (19)$$

that the single phase AC grid power Pg balances the power fluctuation of the photovoltaic source Ppv thus a constant charge power, PB, is obtained at the ESS. For EV battery charging using both the single phase AC

grid and the photovoltaic power, the direction of the AC grid current ig changes to negative while drawing power from the grid. The inverter side can be operated bidirectionally and the PV and the grid provides power for the charger, maintaining the power balance.

$$v_{PV}i_{PV} + i_{grms}v_{grms} = v_b i_b \qquad (20)$$

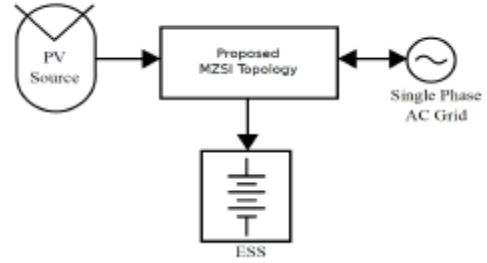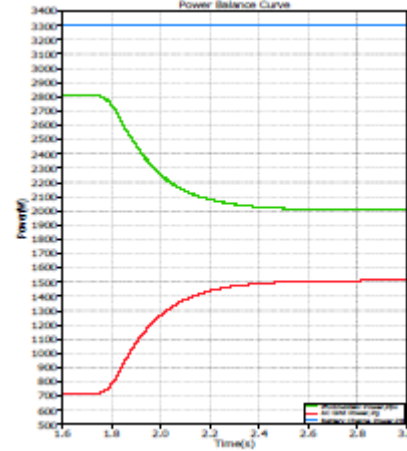
Fig. 6. Simplified Block Diagram of the System

Fig. 7. Simulation Waveform for the power balance between thePhotovoltaic input power, the AC Grid side and the battery power.

Photovoltaic input power, the AC Grid side and the battery power As long as the voltage across the input capacitor Cin is maintained to atleast the minimum value of the PV voltage, the MZSI can be operated as a grid connected rectifier/charger in the absence of the PV [15]-[16]. Anti-islanding protection

61

techniques for the ZSI topology have been addressed in literature previously in [17].

IV. SIMULATION AND EXPERIMENTAL RESULTS

A. Simulation study for a MZSI operation

The simulation studies to demonstrate the behaviour of the proposed topology have been carried out using PLECS 4 for a 3.3 kW charger for a string inverter configuration. Simulation has been carried out for the system shown in Fig.2 Fig.7 shows at simulation time t=1.75 s, the input PV power reduces from 2.8 kW to 2 kW, the grid power increases from 710 W to 1500 W to maintain the output charger power to 3.3kW and the corresponding grid current, DC link voltage, capacitor voltage and the battery current is shown in Fig.8.
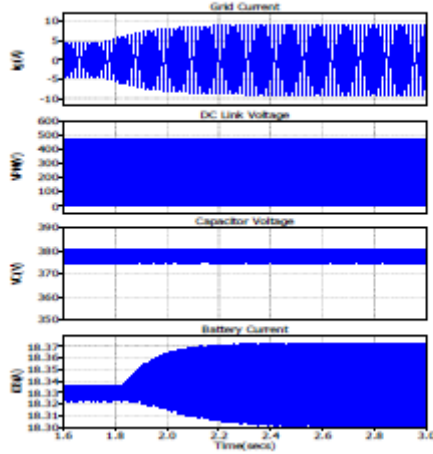

Fig. 8. SimulationWaveform of the grid current,Ig, DC link voltage,VPN, Capacitor Voltage,VC1, and Battery current,ib for the power balance between the Photovoltaic input power, the AC Grid side and the battery power.

TABLE I MODIFIED ZSI BASED CHARGER SYSTEM SIMULATION SPECIFICATIONS

Parameters	Value
Input Voltage, V_{in}	286 V
Input Current, I_{in}	9.8 A
Inductor Value, $L_1 = L_2$	500 uH
ZSI Switching Frequency, F_{SW}	25 kHz
Grid Voltage (RMS), V_g	240 V
Inverter Output Filter Inductor, L_f	7.5 mH
PV Input Power, P_{PV}	2.8 kW
Input Capacitor, C_{in}	2 mF
HBC Switching Frequency, f	50 kHz
HBC Output Filter, L_B	1 mH
Battery charge power, P_B	3.3 kW

TABLE II COMPONENT MODELS USED FOR LOSS MODELING OF THE PROPOSED SYSTEM

Component	Value
Diode, D	STTH6010W
ZSI MOSFETs [S_A, S_B, S_C and S_D]	APT28M120L
HBC MOSFETs [S_{AHB}, S_{BHB}, S_{CHB} and S_{DHB}]	APT28M120L
HBC Diodes, [S'_{AHB}, S'_{BHB}, S'_{CHB} and S'_{DHB}]	STTH6010W
Capacitor, C_{in}, C_1 and C_2	ECE-T2VP182EA

B. Loss Modeling

The loss modeling for the proposed system shown in Fig. 2 has been carried out by modeling the actual components in PLECS 4.0. The switching components used for the modeling is shown in the Table II, For the loss modeling of the passive components, the internal resistance of the inductors, L1, L2 and Lf are r=100 m and the ESR, RHB for the capacitors C1, C2 and Cin

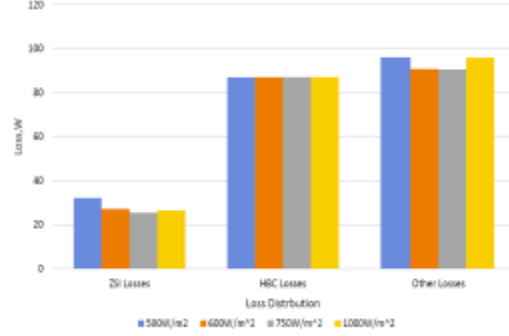

Fig. 9. Loss distribution chart for the MZSI topology for a fixed charging power PB=3.3 kW at 25 _C, under varying irradiation
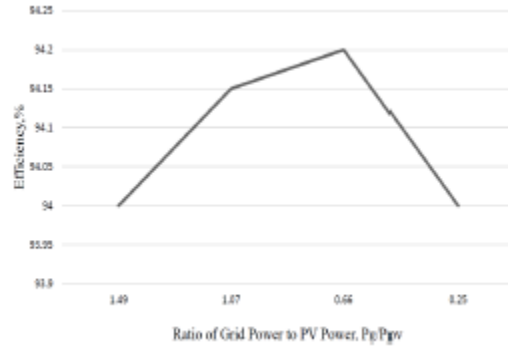

Fig. 10. Efficiency curve for different ratios of AC Grid Power Pg to Photovoltaic Power Ppv curve for a fixed charging power PB=3.3 kW at 25 _C under varying irradiation are 138 m.

Fig. 9 shows the loss distribution between the ZSI (conduction and switching losses of the MOSFETs and diode D), the HBC (conduction and switching losses of the MOSFETs and secondary diodes) and other losses in due to the inductor, capacitors, leakage losses in the high frequency transformer and battery series resistances in the system for varying irradiations for a constant charging power PB=3.3 kW. Fig. 10 shows the efficiency is around 94% from the efficiency curve for various ratios of AC Grid Power,Pg, to Photovoltaic Power, Ppv for a fixed charging power, PB=3.3 kW at 25 _C, for varying irradiation between 500W=m2 to 1000W=m2. Although the efficiency variations is small, the efficiency is the highest when the sharing between the photovoltaic power Ppv and the grid power Pg is

equal. For a constant frequency of operation,the HBC MOSFET losses remain constant for a fixed value VB and charging power,PB. Although in reality, this might not be the case. The efficiency of the converter will change with the change in the battery voltage. Fig. 11 shows the distribution of the losses beween the ZSI losses,the HBC MOSFETs and the losses due
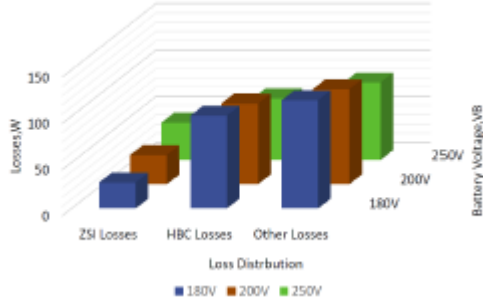

Fig. 11. Loss distribution for various battery voltages,VB, for a fixed charging power,PB=3.3 kW, at 45 _C

TABLE III MODIFIED ZSI BASED CHARGER SYSTEM PROTOTYPE ELECTRICAL SPECIFICATIONS

Parameters	Value
Input Voltage, V_{in}	38 V
Input Current, I_{in}	3.82 A
Inductor Value, L_1 & L_2	500 uH
Peak DC Link Voltage, V_{PN}	63.33 V
Modulation Index, M	0.75
Shoot Through Duty Ratio, D_{0MAX}	0.2
Switching Frequency, F_{SW}	25 kHz
Grid Voltage, V_g	34 V(RMS)
Inverter Output Filter Inductor, L_f	2.5 mH
HBC switching frequency, f_{HBC}	50 kHz

transformer and battery series resistances in the system for various battery voltages. From Fig.11,at 45 _C, the vpv drops to 258V and it can be observed that with the increase in battery voltage the ZSI losses increase but the HBC losses and the losses in the passive components reduce.

C. Experimental Verification of the MZSI power balance operation

In this paper as proof of concept, a scaled down 175W experimental setup was built using MATLAB/Simulink and
dSPACE 1103.The setup has the following specifications shown in table III. Fig. 12 shows the PWM scheme for the HBC. Each of the split primary operate for half the HBC switching period. Each MOSFET SAHB, SBHB, SCHB and SDHB operates exclusively for one quarter of the entire HBC switching period. Equation (23) can be written in terms of the current sharing between the AC load(grid) and the battery as:

$$i_{PV} = \frac{1 - D_0}{2(1 - 2D_0)}i_b + \frac{M}{\sqrt{2}(1 - 2D_0)}i_g \qquad (21)$$

where M is the modulation index and D0 is the shoot through duty ratio. For D0=0.2,

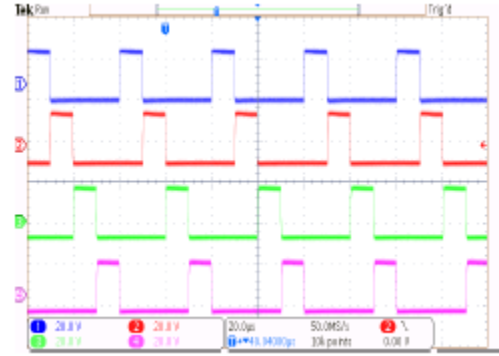$$i_{PV} = \frac{2}{3}i_b + \frac{\sqrt{3}}{2}i_g \qquad (22)$$

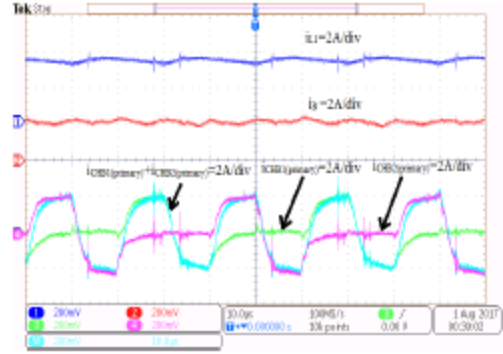Fig. 12. PWM logic for the isolated HBC

Fig. 13. Experimental setup waveforms for the Inductor current(top), charger output current(middle) and the primary currents of the split charger(bottom)

From equation (22), at D0=0.2, for an input current iPV =3.82 A and fixed HBC output current ib=2 A, the ZSI AC output current ig is calculated to be 2.87 A. Fig.13 shows the the inductor current iL1, the battery current iB and the split primary current iCHB1 and iCHB2 and the total primary current. Each of the primary operate alternately. The total primary current is a high frequency alternating current of fHBC=50 kHz. From Fig. 13 and Fig. 14, the charger ouput current is maintained at 2 A using a Chroma Programmable AC/DCElectronics Load(Model 6304). The PV input current is maintained at 3.82 A using a Magna-power LXITM solar emulator. The output grid current is observed to be 2.66 A. Fig. 15 shows the experimental setup for the proof of concept. The lower values of the output current is a result of the losses in the circuit. The practical PI values for the ACside current control was KP =0.03 and the battery loop was KPB=.0003 and KIB=.09 and the input PV current loop were KPin=0.005 and KIin=2.
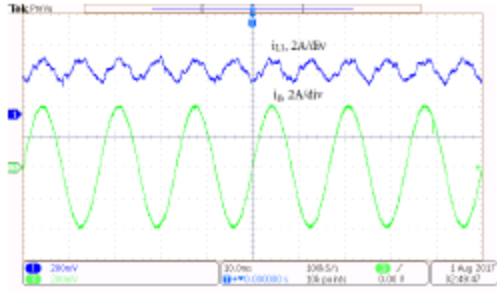
Fig. 14. Experimental waveform input current(blue) and output current(green) between the charger and the AC output of the MZSI
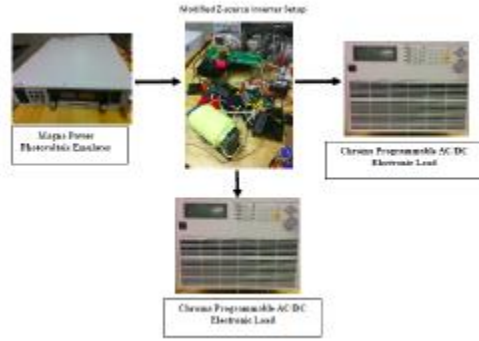

Fig. 15. Experimental setup

Table Iv Isolated Half Bridge Dc-Dc System Electrical Specifications

Parameters	Value
Input Voltage, V_C	50.667 V
Output Voltage , V_B	25.335 V
Switching Frequency, $F_{sw(H B}$	50 kHz
Filter inductor, L_B,	330 uH

V. CONCLUSION

A modified ZSI topology has been proposed in this paper is an attractive solution for photovoltaic grid connected charging systems. It consist of a single stage photovoltaic grid (PV-Grid) connection and an integrated charger for PV-Grid connected charging or energy storage. This topology can be applied to centralized configuration for charging in semi-commercial locations such as a parking lot of a shopping mall. For residential applications, this idea can be extended to string inverters with the charger side of the string inverter configurations connected in series or parallel for current sharing. The paper proposes a an energy storage topology using Z source converter through symmetrical operation of its impedance network.

REFERENCES

[1] D. Aggeler, F. Canales, H. Zelaya, D. L. Parra, A. Coccia, N. Butcher, and O. Apeldoorn, "Ultra-fast dc-charge infrastructures for ev-mobility and future smart grids," in Proc. of IEEE PES Innovative Smart Grid Technologies
Conference Europe, pp. 1–8, Oct. 2010.
[2] G. Carli and S. S. Williamson, "Technical considerations on power conversion for electric and plug-in hybrid
electric vehicle battery charging in photovoltaic installations," IEEE Trans. on Ind. Electron., vol. 28, no. 12,
pp. 5784–5792, 2013.
[3] J. G. Ingersoll and C. A. Perkins, "The 2.1 kw photovoltaic electric vehicle charging station in the city of santa monica, california," in Proc. of the Twenty Fifth IEEE Photovoltaic Specialists Conference, pp. 1509– 1512, May. 1996.
[4] S. B. Kjaer, J. K. Pedersen, and F. Blaabjerg, "A review of single-phase grid-connected inverters for photovoltaic modules," IEEE Trans. on Ind. Appl., vol. 41, no. 5, pp. 1292–1306, Sep. 2005.
[5] N. A. Ninad, L. A. C. Lopes, and I. S. Member, "Operation of Single-phase Grid-Connected Inverters with Large
DC Bus Voltage Ripple," Proc. of the IEEE Canada Electrical Power Conference, 2007.
[6] S. Bai, D. Yu, and S. Lukic, "Optimum design of an ev/phev charging station with dc bus and storage system,"
in Proc. of IEEE ECCE, pp. 1178–1184, Sep. 2010.
[7] F. Z. Peng, "Z-Source Inverter," in IEEE Trans. on Ind. Appl., vol. 39, no. 2, pp. 504–510, 2003.
[8] Y. Huang, M. Shen, F. Z. Peng, and J. Wang, "Zsource inverter for residential photovoltaic systems," IEEE Trans. on Power Electron., vol. 21, no. 6, pp. 1776–1782, Nov. 2006.
[9] S. A. Singh, N. A. Azeez, and S. S. Williamson, "Capacitance reduction in a single phase quasi z-source inverter
using a hysteresis current controlled active power filter,"in in Proc. of IEEE 25th Int. Symp.on Ind. Electron., pp.
805–810, Jun. 2016.
[10] S. A. Singh, G. Carli, N. A. Azeez, and S. S. Williamson,"A modified z-source converter based single phase
pv/grid inter-connected dc charging converter for future transportation electrification," in Proc. of IEEE ECCE,
pp. 1–6, Sep. 2016.
[11] Y. Li, S. Jiang, J. G. Cintron-Rivera, and F. Z. Peng, "Modeling and control of quasi-z-source inverter for
distributed generation applications," IEEE Trans. on Ind.Electron., vol. 60, no. 4, pp. 1532–1541, Apr. 2013.

[12] T. Chandrashekhar and M. Veerachary, "Control of single-phase z-source inverter for a grid connected system,"
in Proc. of Int. Conf. on Power Syst., pp. 1–6, Dec.2009.

[13] B. Ge, Y. Liu, H. Abu-Rub, R. S. Balog, F. Z. Peng,S. McConnell, and X. Li, "Current ripple damping control
to minimize impedance network for single-phasequasi-z source inverter system," IEEE Trans. on Ind. Info., vol. 12, no. 3, pp. 1043–1054, Jun. 2016.

[14] B. Ge, H. Abu-Rub, F. Z. Peng, Q. Lei, A. T. de Almeida, F. J. T. E. Ferreira, D. Sun, and Y. Liu, "An energy-stored quasi-z-source inverter for application to photovoltaic power system," IEEE Trans. on Ind. Electron., vol. 60,
no. 10, pp. 4468–4481, Oct. 2013.

[15] J. Rabkowski, R. Barlik, and M. Nowak, "Pulse width modulation methods for bidirectional/high-performance
z-source inverter," in Proc. of IEEE Power Electron.Spec. Conf., pp. 2750–2756, Jun. 2008.

[16] S. Dong, Q. Zhang, and S. Cheng, "Analysis of critical inductance and capacitor voltage ripple for a bidirectional z -source inverter," IEEE Trans. on Power Electron.,vol. 30, no. 7, pp. 4009–4015, Jul. 2015.

[17] M. Trabelsi and H. Abu-Rub, "A unique active antiislanding protection for a quasi-z-source based power conditioning system," in Proc. of IEEE Appl. Power Electron. Conf.e and Expo., pp. 2237–2243, Mar. 2015